$GABA_A$ Receptor Kinetics in the Cerebellar Nuclei: Evidence for Detection of Transmitter from Distant Release Sites

Jason R. Pugh* and Indira M. Raman*†
*Institute for Neuroscience and †Department of Neurobiology and Physiology, Northwestern University, Evanston, Illinois

ABSTRACT Neurons of the cerebellar nuclei receive GABAergic input from Purkinje cells. Purkinje boutons have several closely spaced presynaptic densities without GABA transporters, raising the possibility that neurotransmitter released by one presynaptic site diffuses to multiple postsynaptic sites. To test whether such local spillover may contribute to transmission, we studied gating of $GABA_A$ receptors at 31–33°C in cerebellar nuclear neurons acutely dissociated from mice. Currents were evoked by rapid application of long steps, brief pulses, and high-frequency trains of GABA to outside-out patches. Receptors desensitized and deactivated rapidly, and dose-response measurements estimated an EC_{50} of ~30 μM. From these data, a kinetic scheme was developed that replicated the recorded currents. Next, we simulated diffusion of GABA in the synaptic cleft, constrained by previous electron microscopic data, and drove the kinetic $GABA_A$ receptor model with modeled concentration transients. Simulations predicted receptor occupancies of ~100% directly opposite the release site and ~50% at distant postsynaptic densities, such that receptors up to 700 nm from a release site opened on the timescale of the inhibitory postsynaptic currents before desensitizing. Further simulations of probabilistic release from multiple-site boutons suggested that local spillover-mediated transmission slows the onset and limits the extent of depression during high-frequency signaling.

INTRODUCTION

The synapse between Purkinje cells and neurons of the cerebellar nuclei is typified by high-frequency inhibitory transmission. During cerebellar activities, presynaptic neurons fire at rates exceeding 50 Hz (Thach, 1968), eliciting inhibitory postsynaptic currents (IPSCs) that are subject to a moderate short-term depression (Telgkamp and Raman, 2002). We previously investigated why IPSCs at corticonuclear synapses depress by only ~50% at stimulation frequencies of 100 Hz, even though the expected depletion of presynaptic vesicles predicts a much greater depression. Ultrastructural studies indicated that the terminal boutons of Purkinje axons have multiple synaptic densities, suggestive of several release sites per bouton. These densities are not separated by GABA transporters; instead, transporters are located exclusively in astrocytic processes surrounding boutons. These structural features raised the possibility that transmitter released from a presynaptic active zone might diffuse to receptors at many of the postsynaptic densities apposed to that bouton. Electrophysiological and modeling studies supported this idea, suggesting that corticonuclear synapses are well adapted for local spillover, i.e., restricted to sites under each astrocytically ensheathed bouton, and that this spillover-mediated transmission may minimize depression (Telgkamp et al., 2004).

The efficacy of spillover-mediated transmission, however, necessarily depends on the properties of postsynaptic receptors. Specifically, the diffusion distance from a presynaptic release site to a distant postsynaptic density is likely to be a few hundred nanometers, raising the question of whether the affinity and gating kinetics of those distant postsynaptic receptors allow channel opening on the timescale of the IPSC. Moreover, either brief applications of high doses or prolonged exposure to low doses of ligand lead to desensitization of $GABA_A$ receptors of most neurons (Jones and Westbrook, 1995; Galarreta and Hestrin, 1997; Zhu and Vicini, 1997; Mellor and Randall, 1998; Perrais and Ropert, 1999; Overstreet et al., 2000; Mozrzymas et al., 2003). If, in response to GABA diffusing from distant release sites, $GABA_A$ receptors tend to desensitize rather than open, then any spillover that occurs may intensify rather than minimize depression. Despite the unequivocal observation that receptors desensitize in response to exogenously applied GABA, however, the extent of desensitization that occurs in response to synaptically released transmitter appears variable: At some synapses, desensitization is undetectable (Mellor and Randall, 2001), whereas at other synapses, the evidence for desensitization is strong (Overstreet et al., 2000; Kirischuk et al., 2002).

In the present study, we used rapid application of GABA to outside-out patches from isolated neurons at 31°–33°C to describe the gating properties of $GABA_A$ receptors in the cerebellar nuclei. These data were used to develop a kinetic model of the receptors, which was then driven by simulations of the concentration transients that result from transmitter release from multiple-site boutons. This approach allowed us to predict responses of postsynaptic receptors at distances as far as 700 nm from the site of GABA release. The results suggest that, although a substantial fraction of $GABA_A$ receptors are likely to desensitize during high-frequency

Submitted November 5, 2004, and accepted for publication December 14, 2004.

Address reprint requests to Indira M. Raman, Dept. of Neurobiology and Physiology, 2205 Tech Drive, Northwestern University, Evanston, IL 60208. Tel.: 847-467-7912; Fax: 847-491-5211; E-mail: i-raman@northwestern.edu.

0006-3495/05/03/1740/15 $2.00

doi: 10.1529/biophysj.104.055814

synaptic activity, receptors activated by spillover-mediated transmission at corticonuclear synapses can contribute significantly to the peak of the IPSC.

MATERIALS AND METHODS

Preparation of isolated neurons

Neurons of the cerebellar nuclei were isolated from 13- to 16-day-old C57BL6 mice (Charles River, Wilmington, MA) as described previously (Raman et al., 2000; Afshari et al., 2004). In accordance with institutional guidelines, mice were deeply anesthetized with halothane and decapitated. The cerebellum was removed and placed in cold (4°C) Tyrode's solution (150 mM NaCl, 4 mM KCl, 2 mM $CaCl_2$, 2 mM $MgCl_2$, 10 mM HEPES, and 10 mM glucose, pH 7.4). Parasagittal slices of the cerebellum were cut on a tissue chopper (Mickle Laboratory Engineering, Gomshall, UK). Slices were incubated for 20 min at 31°C in a dissociation solution consisting of minimal essential medium (MEM; Invitrogen, Carlsbad, CA), 10 mM HEPES, 2 mM cysteine, and 1 mM EDTA (pH 7.2 with NaOH), to which 40 U/ml papain (Worthington, Lakewood, NJ) and 1 U/ml chondroitinase ABC (Glyco, San Leandro, CA) were added. After enzymatic treatment, the slices were washed in the MEM-based solution, without enzymes, but including 1 mg/ml bovine serum albumin and 1 mg/ml trypsin inhibitor. The cerebellar nuclei were microdissected out of the slices and triturated using fire-polished Pasteur pipettes. Isolated neurons were allowed to settle in Tyrode's solution for 1 h before recording. Drugs were from Sigma-Aldrich (St. Louis, MO) unless noted.

Electrophysiological recordings and analysis

Voltage-clamp recordings were made with an Axopatch 200B amplifier (Axon Instruments, Foster City, CA), sampled at 20 kHz and filtered at 5 kHz. Borosilicate recording pipettes (1.5–3 MΩ open tip resistance) were filled with an internal solution containing 117 mM K-gluconate, 5.4 mM NaCl, 3.6 mM Na-gluconate, 1.8 mM $MgCl_2$, 9 mM EGTA, 9 mM HEPES, and 4.5 mM sucrose, 14 mM Tris-creatine phosphate, 4 mM MgATP, and 0.3 mM Tris-GTP, pH 7.4, with KOH. Except as noted, recordings were made from outside-out or nucleated patches held at 0 mV, to give a Cl^- driving force of 70 mV. External solutions were applied through a θ-glass pipette mounted on an LSS-3000 ultrafast solution-switching piezoelectric device (EXFO Burleigh, Victor, NY). The control solution consisted of Tyrode's solution diluted by 2% with purified water (to create a detectable junction potential for measurement of exchange times), and the test solution contained GABA or baclofen dissolved in Tyrode's solution. External solutions were driven through the θ-glass pipette with either a syringe pump (Thermo Orion, Waltham, MA) or a pressure perfusion system (AutoMate Scientific, San Francisco, CA). Because of reports that factors released from Tygon tubing can block $GABA_A$ receptors (Wagner and Jones, 2004), Tygon was eliminated from the flow system. Complete exchange from the control to the test solution, measured by the change in open-tip junction potential, was accomplished in 336 ± 13 μs. The recording chamber rested on a heating plate (Fryer, Huntington, IL) to maintain the cells at elevated temperatures. Submersion of the θ-glass served to heat the external solutions, and GABA-mediated currents were confirmed to have been recorded between 31° and 33°C. Data were analyzed with IGOR-Pro software (Wavemetrics, Lake Oswego, OR) and results are presented as mean ± SE.

Modeling

The kinetics of GABA-mediated currents recorded from cerebellar nuclear neurons were modeled in NEURON (Hines and Carnevale, 1997), with an initial scheme based on the model of Jones and Westbrook (1995). States were added and rate constants were optimized, while accounting for detailed balance, to replicate the macroscopic properties of receptors in patches.

The spread of GABA in the synaptic cleft was modeled as diffusion in an infinite disk (Otis et al., 1996). Parameters for cleft width (set at 14 nm) and number of molecules per vesicle (set at 2500) were identical to those of Telgkamp et al. (2004), but the diffusion coefficient was reduced from of 0.5 μm^2/ms to 0.37 μm^2/ms, based on data from Nielsen et al. (2004). The concentration of GABA was simulated at multiple times from 10 μs to 10 ms after release, at distances 0, 250, 350, 500, 550, and 700 nm lateral to the site of GABA release. These values, which are approximately equal to 250 multiplied by 0, 1, $\sqrt{2}$, 2, $\sqrt{5}$, and $2\sqrt{2}$, represent all possible distances between pairs of sites in a regular 3 × 3 array with a minimal intersite distance of 250 nm. The data points were fitted piecewise with arbitrary polynomial functions, which were then used as concentration functions to drive the kinetic model of $GABA_A$ receptors.

For the multiple-site model of Figs. 7 and 8, GABA release from boutons was simulated by modifying the model of Telgkamp et al. (2004) to keep track of the particular sites that released on each stimulation in a 10-pulse, 100-Hz train. Procedures were written and executed in IGOR-Pro. Boutons were modeled as a 3 × 3 array of nine release sites, and simulations began with 100% occupancy of presynaptic sites. For each stimulus, a random value between 0 and 1 was generated for each site. If the random value was less than the vesicular release probability and if the site was occupied, that site was recorded as having released. Depleted sites were randomly replenished according to a double-exponential function, with a fast τ of 150 ms (accounting for 50% of replenishment) and a slow τ of 15 s.

RESULTS

Our previous studies have led to the hypothesis of a local, effective, spillover-mediated transmission that serves to minimize short-term synaptic depression at corticonuclear synapses (Telgkamp et al., 2004). The present experiments were directed toward testing, first, whether $GABA_A$ receptors of cerebellar nuclear neurons can be activated by GABA released from relatively distant presynaptic sites, and second, whether desensitization of receptors is likely to influence short-term depression. Addressing these questions required a method to predict the gating of synaptic receptors during high-frequency trains of complex concentration transients of GABA similar to those that normally occur during corticonuclear activity. To this end, we recorded GABA-activated currents from cerebellar nuclear neurons and developed a kinetic model of the $GABA_A$ receptors that replicated the experimentally measured responses.

Desensitization of $GABA_A$ receptors in the cerebellar nuclei

$GABA_A$-receptor mediated currents in outside-out patches excised from acutely dissociated cerebellar nuclear neurons were recorded at 31°–33°C, to maximize their applicability to previous data recorded at similar temperatures in cerebellar slices. Patches were held at 0 mV, for a 70-mV driving force on Cl^-, and currents were evoked by rapid application of GABA to each patch. In response to a 100-ms application of 1 mM GABA (Fig. 1 *A*, *left*), currents activated in <0.5 ms and desensitized with a dominant fast time constant (τ_{fast}) of ~3 ms and a slow time constant

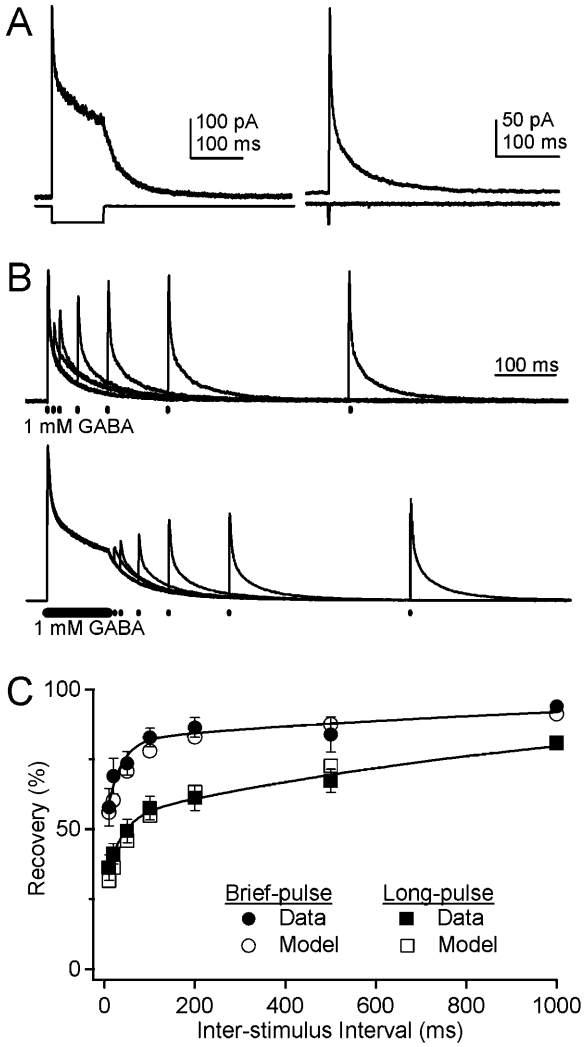

FIGURE 1 Desensitization, deactivation, and recovery of $GABA_A$ receptors in cerebellar nuclear neurons. (*A*) Current evoked from an outside-out patch by a 100-ms (*left*) and 1-ms (*right*) application of 1 mM GABA. Traces below each recording represent the time course of GABA application as determined by the change in open-tip junction potential. (*B*) Six overlaid traces illustrating recovery from desensitization evoked by a 1-ms (*top*) or a 100-ms (*bottom*) application of GABA. *Bars* indicate duration of agonist exposure. Intervals, 10–1000 ms. Recovery pulse, 1 ms. (*C*) Peak test currents normalized to the peak conditioning current, plotted versus recovery interval (*solid symbols*, as labeled). Data were fit with a double-exponential function (see Table 1). Simulated data from the kinetic model of $GABA_A$ receptors in patches are plotted as *open symbols*.

TABLE 1 Concentration-dependence and kinetic parameters of experimentally recorded and simulated $GABA_A$ receptors

	Data	Model
Activation (10–90%) ($N = 17$)	475 ± 28 μs	175 μs
Desensitization (100-ms pulse) ($N = 52$)		
τ_{fast}	3.2 ± 0.18 ms	3.2 ms
% τ_{fast}	60.8 ± 2.1%	67.0%
τ_{slow}	56.3 ± 3.1 ms	68.3 ms
% steady-state current*	37.6 ± 1.3%	28.1%
Deactivation (100-ms pulse) ($N = 38$)		
τ_{fast}	24.7 ± 1.4 ms	25.2 ms
% τ_{fast}	59.1 ± 2.3%	61.3%
τ_{slow}	94.2 ± 5.5 ms	76.6 ms
Deactivation (1-ms pulse) ($N = 18$)		
τ_{fast}	4.0 ± 0.47 ms	3.4 ms
% τ_{fast}	68.5 ± 1.8%	60.4%
τ_{slow}	42.8 ± 2.5 ms	34.6 ms
Brief-pulse recovery ($N = 5$–6)†		
τ_{fast}	31 ms	49.3 ms
% τ_{fast}	55%	56.6%
τ_{slow}	1238 ms	1235 ms
Long-pulse recovery ($N = 5$–8)†		
τ_{fast}	34.7 ms	67 ms
% τ_{fast}	28.5%	41.2%
τ_{slow}	1222 ms	1329 ms
Max value dose-response ($N = 4$–7)†		
EC_{50}	38.4 μM	28 μM
Hill coefficient	0.64	0.89
1-ms value dose-response ($N = 4$–7)†		
EC_{50}	145.4 μM	87.7 μM
Hill coefficient	1.2	1.8

*100 × (*Current amplitude at end of 100-ms GABA application*)/(*Peak current amplitude*).
†Number of cells at each point.

(τ_{slow}) of ~56 ms (Table 1). Upon removal of GABA, currents deactivated bi-exponentially, with time constants of ~25 and ~100 ms (Table 1). With 1-ms applications of GABA, current decayed only slightly during the pulse. Upon removal of GABA, however, deactivation was more rapid than after a long pulse (Jones and Westbrook, 1995), with time constants that closely resembled those of desensitization (Fig. 1 *A*, *right*, Table 1). The $GABA_B$ agonist baclofen evoked currents that were only 2.4 ± 1.0% of the total current evoked by 1 mM GABA ($N = 3$ paired observations), consistent with little $GABA_B$-receptor-activated inward rectifier current flowing at 0 mV (Sodickson and Bean, 1996). These results suggest that the currents were mediated primarily by $GABA_A$ receptors.

The similarity between the time courses of desensitization during long pulses and deactivation after brief pulses raises the possibility that the decay upon removal of GABA may represent receptors entering desensitized states (Galarreta and Hestrin, 1997). To test for such ''brief-pulse desensitization'' (Hestrin, 1992; Colquhoun et al., 1992; Raman and Trussell, 1995), we recorded responses to pairs of 1-ms pulses of 1 mM GABA (Fig. 1 *B*, *top*). Although macroscopic desensitization during the first pulse was minimal, a second pulse applied after a 10-ms interstimulus interval evoked a current whose peak (measured relative to the baseline preceding the first pulse) was only 58 ± 7% of the first response, indicating that receptors continued to desensitize after the initial application of GABA. Although this tendency for brief-pulse desensitization suggests that at least some receptors may desensitize during synaptic stimulation, the extent to which desensitization influences response amplitudes evoked by trains of presynaptic stimuli

will depend largely on the time course of recovery from desensitization. We therefore assessed the rate of recovery after a 1-ms conditioning pulse with 1-ms test pulses at intervals ranging from 10 to 1000 ms (Fig. 1 *B*, *top*). The amplitude of the responses to each test pulse, normalized to the response to the conditioning pulse, was plotted against the interstimulus interval, indicating that recovery had a relatively rapid phase, yielding an availability of receptors of ~80% within 100 ms, as well as a slow phase (Fig. 1 *C*, *solid circles,* $N = 6$). Parameters of a double-exponential fit to recovery are given in Table 1. When receptors were conditioned with longer (100-ms) pulses of GABA, the extent of desensitization was greater and the rate of recovery was slower (Fig. 1 *B*, *bottom*). Recovery from long-pulse desensitization could be fit with a double-exponential function with time constants that were similar to those of recovery from brief-pulse desensitization, but with a more heavily weighted slow component (Fig. 1 *C*, *solid squares,* $N = 5$; Table 1).

Dose-response of $GABA_A$ receptors

Since the sensitivity of postsynaptic receptors to GABA is likely to be a central factor regulating the contribution of spillover to the total IPSC, we measured the dose-response relationship for $GABA_A$ receptors of cerebellar nuclear cells. Each patch was exposed for 100 ms to GABA at 1 mM and at least one other concentration between 10 μM and 10 mM (Fig. 2 *A*). Maximal currents evoked by each concentration were normalized to the maximal response to 1 mM GABA, and the dose-response data were fitted with a Hill equation, which estimated the EC_{50} to be 38 μM (Fig. 2 *B*, *solid circles;* Table 1). To test whether patch excision changed the sensitivity of the receptors to GABA, we repeated the experiment in whole cells. Although rapid solution exchange is likely to be somewhat compromised in these recordings, the whole-cell data fell within the standard deviations for the patch data. Fitting the mean values estimated a slightly lower EC_{50} for whole cells (23 μM) than for patches, a difference that is consistent with the expected underestimate of peak amplitudes at the highest concentrations of agonist (Fig. 2 *B*, *open triangles*). Taking the whole cell and patch data together suggests that a reasonable estimate of the EC_{50} for peak responses to GABA is ~30 μM (see Discussion). Since synaptic exposure to neurotransmitter is likely to be brief (e.g., Clements et al., 1992; Diamond and Jahr, 1995), we also measured the non-equilibrium dose-response curve in patches as the response at each concentration after 1 ms of GABA application. Under these conditions, the EC_{50} (145 μM) was considerably lower than for the peak currents (Fig. 2 *B*, *solid squares;* Table 1).

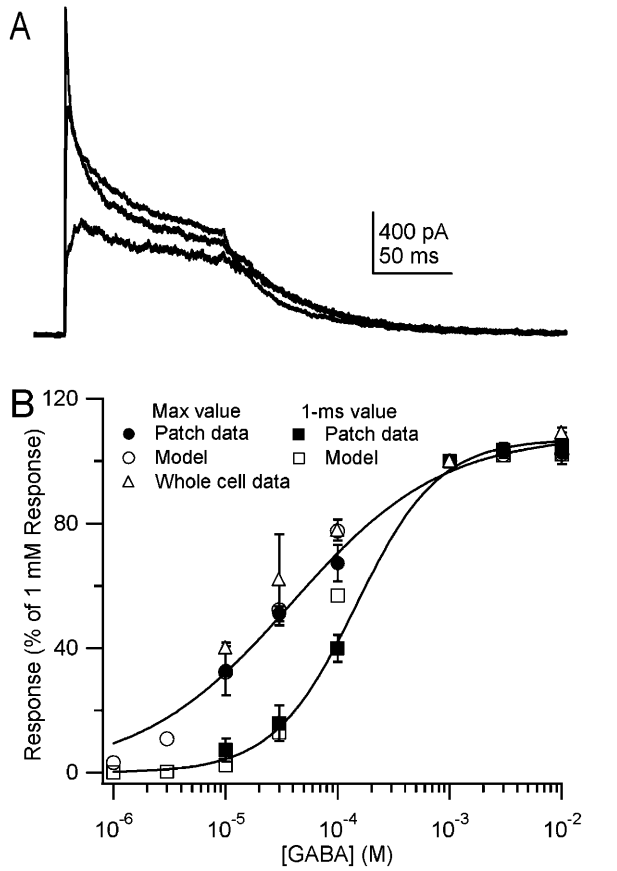

FIGURE 2 Dose-response relationship for $GABA_A$ receptors. (*A*) Currents evoked by 100-ms applications of 1 mM, 100 μM, and 10 μM GABA to a single outside-out patch. The peak current amplitude increased with concentration. (*B*) Dose-response relationship for peak currents evoked by GABA in outside-out patches (*solid circles*) and whole cells (*open triangles*), as well as in simulations from the kinetic model of $GABA_A$ receptors in patches (*open circles*). The non-equilibrium dose-response relation taken as the current amplitude after 1 ms of GABA application in patches (*solid squares*) and simulations (*open squares*) are also shown. *Lines* represent fits to the data using the Hill equation (see Table 1).

Development of a kinetic model

The rates of activation, deactivation, desensitization, and recovery from desensitization, as well as the concentration-dependence of responses to GABA, were used as parameters to develop a kinetic model of gating by $GABA_A$ receptors of cerebellar nuclear neurons. In the model (Fig. 3), which was modified from the kinetic scheme of Jones and Westbrook (1995), receptors can bind two molecules of agonist (*A*), leading to singly- or doubly-liganded closed (*C*), open (*O*), and desensitized (*D*) states. In response to rapid application of GABA, most of the current results from occupancy of OA_2, with a small contribution of OA at low concentrations of GABA. Based on the bi-exponential onset of desensitization, we included two doubly-liganded desensitized states, the fast (DA_2f) and slow (DA_2s) desensitized states (Trussell and Fischbach, 1989; Galarreta and Hestrin, 1997). In this scheme, fast macroscopic desensitization results primarily from transitions into DA_2f, with the slow phase resulting from entry into DA_2s. To account for the slow component of

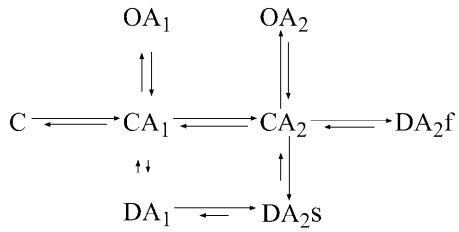

FIGURE 3 Kinetic scheme for $GABA_A$ receptor gating. *C* denotes a closed state; *O*, an open state; *D*, a desensitized state; and *A*, a molecule of agonist, with subscripts indicating the number of agonist molecules bound. The fast and slow desensitized states are labeled *f* and *s*, respectively. *Arrows* are proportional to the log of each rate in the presence of 1 mM GABA. Detailed balance is maintained. Rate constants are given in Table 2.

recovery from DA_2s, we included a direct transition to the high-affinity, singly-liganded desensitized state (DA_1). The final scheme is shown in Fig. 3, in which the lengths of the arrows are proportional to the logarithm of the rate constants; rate constants are given in Table 2. The optimized model replicated nearly all aspects of the responses of the patch receptors (Table 1; Figs. 1 *C* and 2 *B*, *open symbols*), although modification of one transition rate was ultimately required to match the synaptic responses (described below).

Responses of receptors in patches to high-frequency trains of GABA

Next, to replicate as many synaptic conditions as possible while experimentally controlling the application of agonist, we applied trains of brief pulses of GABA to patches, with the goal of estimating the extent of desensitization that might result from stimulation rates typical of corticonuclear synapses. A consideration in this experiment is that the rate at which synaptic receptors are exposed to transmitter depends not only on the presynaptic firing rate, but also on the vesicular release probability (P_v) and the extent of spillover from any presynaptic site to other postsynaptic sites under a given bouton. Specifically, with a presynaptic firing rate of 100 Hz, a low P_v, and no local spillover, a postsynaptic density might be exposed to transmitter at a frequency as low as 5 Hz, whereas with effective spillover, receptors might be exposed to transmitter at 100 Hz. Therefore, we measured responses to trains of 1-ms pulses of GABA applied at several frequencies between these extremes. Since transmitter concentration in synaptic clefts has been estimated to be ~1 mM for 1 ms (e.g., Clements et al., 1992), we chose 1 mM as the high end of the concentration range; since the peak concentration at distant receptor sites is likely to be considerably lower (Telgkamp et al., 2004), we repeated all the measurements with 100 μM and 30 μM GABA.

TABLE 2 Rate constants for the kinetic model describing patch responses

Transition	Forward (ms^{-1})	Back (ms^{-1})
C, CA_1	0.04 (μM^{-1})	2
CA_1, CA_2	0.02 (μM^{-1})	4
CA_1, OA_1	0.03	0.06
CA_1, DA_1	0.00033	0.0007
CA_2, OA_2	10	0.4
CA_2, DA_2f	15	0.15
CA_2, DA_2s	1.2	0.006
DA_1, DA_2s	0.015 (μM^{-1})	0.007

Examples of currents evoked by 10-pulse trains are shown in Fig. 4 *A*, for three concentrations of GABA applied at four stimulus frequencies. In response to repetitive stimulation with 1 mM GABA, peak currents (measured relative to the baseline preceding the train) decreased in amplitude at all stimulus frequencies, with the onset of significant desensitization occurring earlier in the train at higher stimulus frequencies. Plotting the normalized total current amplitude against stimulus number, however, illustrated that, regardless of the stimulus frequency, approximately the same degree of desensitization occurred by the 10th response (somewhat >50%; Fig. 4 *B*, *left*). For trains of pulses of 100 μM GABA, the response amplitudes also converged as the trains progressed, although the relative decrement in response amplitude was lower (Fig. 4 *B*, *center*). With trains of 30 μM GABA, however, the peak currents decreased only slightly at the lowest frequency of 5 Hz, and peak currents tended to increase during trains at higher frequencies (Fig. 4 *B*, *right*). These data illustrate that the profile of responses to trains of stimuli depends strongly on the particular concentration of transmitter applied to the receptors. By extension, they suggest that, if neurotransmitter concentration transients are on the order of 1 ms at 100 μM or less, trains of synaptic currents may not show overt evidence of a desensitization-based reduction in response amplitude, even during high-frequency stimulation of receptors that are susceptible to rapid desensitization.

Next, we tested the ability of the model to replicate the patch currents evoked by high-frequency stimulus trains. Simulations of responses to trains at each frequency and agonist concentration are shown in Fig. 5 *A*, and illustrate the good match between the modeled and experimental data. To allow comparison of the relative peak amplitudes, the mean patch responses from Fig. 4 *B* are replotted, along with the simulated responses, against time of stimulation in Fig. 5 *B*. These plots show that the model was effective except under two conditions: First, it failed to reproduce a very slow component of desensitization that occurred with 5-Hz trains of 1-mM GABA, suggesting the existence of ultraslow desensitized states that are lacking in our model; and second, it exaggerated the increase in peak amplitudes of successive responses with 100-Hz applications of 30 μM GABA. Regarding the latter discrepancy, however, the experimental data obtained in the 30-μM, 100-Hz condition was itself somewhat variable, with some patches showing greater apparent facilitation in this condition than others. Despite its shortcomings, the model was largely successful at replicat-

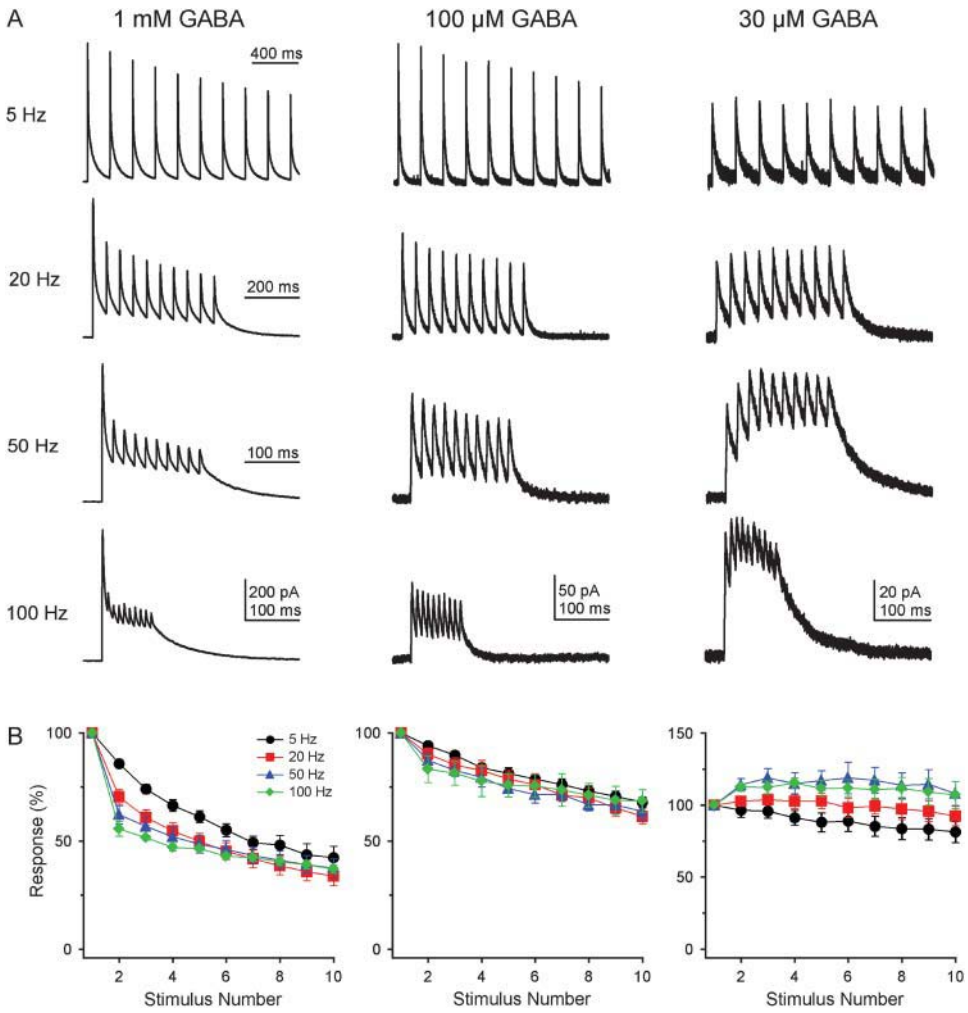

FIGURE 4 Desensitization and summation evoked by trains of pulses of GABA applied to outside-out patches. (*A*) Currents elicited by 10 1-ms pulses of 1 mM, 100 μM, and 30 μM GABA applied to outside-out patches at 5, 20, 50, and 100 Hz. The timescale is the same for each row, and the current scale is the same for each column. The traces at each concentration are from the same patch. Some rundown occurred. (*B*) Mean peak currents, normalized to the first peak in the train, plotted versus stimulus number. For all conditions, *N* ranged from 3 to 12.

ing the experimental data over a wide range of conditions, suggesting that it adequately represented the transitions between the dominant closed, open, and desensitized states of cerebellar nuclear GABA$_A$ receptors in patches. The match between data and simulations appeared sufficient to justify the use of the model to predict the responses of receptors to complex, synapse-like concentration transients of GABA, which could not be recorded experimentally.

Responses of GABA$_A$ receptors to transmitter released from distant release sites

The terminal boutons of Purkinje neurons have several synaptic densities, which appear likely to represent multiple release sites. These boutons also lack GABA transporters, which are instead located exclusively in astrocytes (Chan-Palay, 1977; Ribak et al., 1996; Telgkamp et al., 2004), such that the synaptic densities within a bouton are not isolated by uptake mechanisms. These structural features form the basis of the proposal that Purkinje boutons are adapted for spillover-mediated transmission (Telgkamp et al., 2004). The extent to which spillover-mediated transmission may contribute to the peaks of IPSCs depends on the concentration transient in the cleft, as well as on the properties of the postsynaptic GABA$_A$ receptors. Therefore, with the goal of predicting the responses of GABA$_A$ receptors to transmitter released from a bouton with multiple release sites, we first estimated the concentration transients detected by postsynaptic receptors by simulating transmitter diffusion in the cleft, after release from a multiple-site bouton. The concentration transient detected by receptors at any postsynaptic density will depend on the number of transmitter molecules per vesicle, the diffusion coefficient for the transmitter, and the distance of the receptors from the release site. In our simulations, we assumed 2500 molecules per vesicle (Bruns et al., 2000) and a diffusion coefficient of 0.37 μm^2/ms. This value for the diffusion coefficient is lower than the value used previously (0.5 μm^2/ms, Telgkamp et al., 2004), but is more firmly grounded in experimental data (Nielsen et al., 2004). For a postsynaptic site directly opposite a release site (i.e., 0-nm lateral diffusion), the diffusion distance reduces to

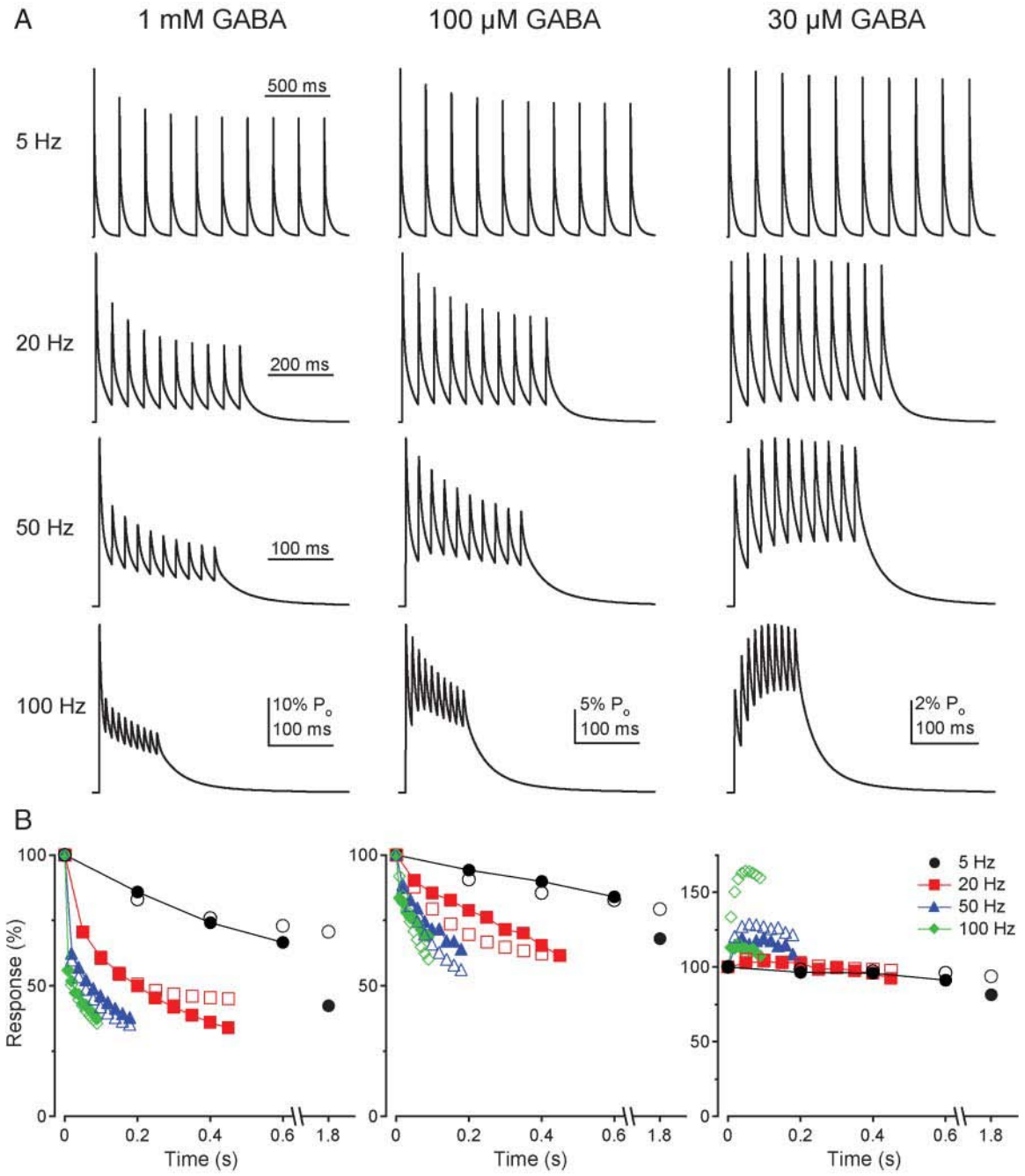

FIGURE 5 Simulated responses to trains of pulses of GABA at different concentrations and frequencies. (*A*) Currents elicited by 10 1-ms pulses of 1 mM, 100 μM, and 30 μM agonist at 5, 20, 50, and 100 Hz simulated by the kinetic scheme of Fig. 3. The timescale is the same for each row, and the *y* scale is open-probability (P_o), and is the same for each column. (*B*) Peak currents, normalized to the peak of the first response, versus time for all stimulus frequencies and concentrations. Experimental data (same as Fig. 4 *B*; *solid symbols*; model data, *open symbols*). Error bars on experimental values are omitted for clarity.

the width of the synaptic cleft, which we have previously measured at 14 nm (Telgkamp et al., 2004). The model predicts that receptors directly opposite a release site will be exposed to a transient of GABA that peaks at 13 mM and decays to 64 μM after 1 ms (Fig. 6 *A*, *left*).

To estimate the responses to release from more distant release sites, we defined a single bouton as a 3 $\times$ 3 array of presynaptic release sites, apposed to a corresponding 3 $\times$ 3 array of postsynaptic sites. Sites were separated by 250 nm from their nearest neighbors (Fig. 6 *B*). The values for the number of release sites per bouton and shortest intersite distance were based on our previous estimates from three-dimensional electron microscopic reconstructions of Purkinje boutons (Telgkamp et al., 2004). With this nine-site

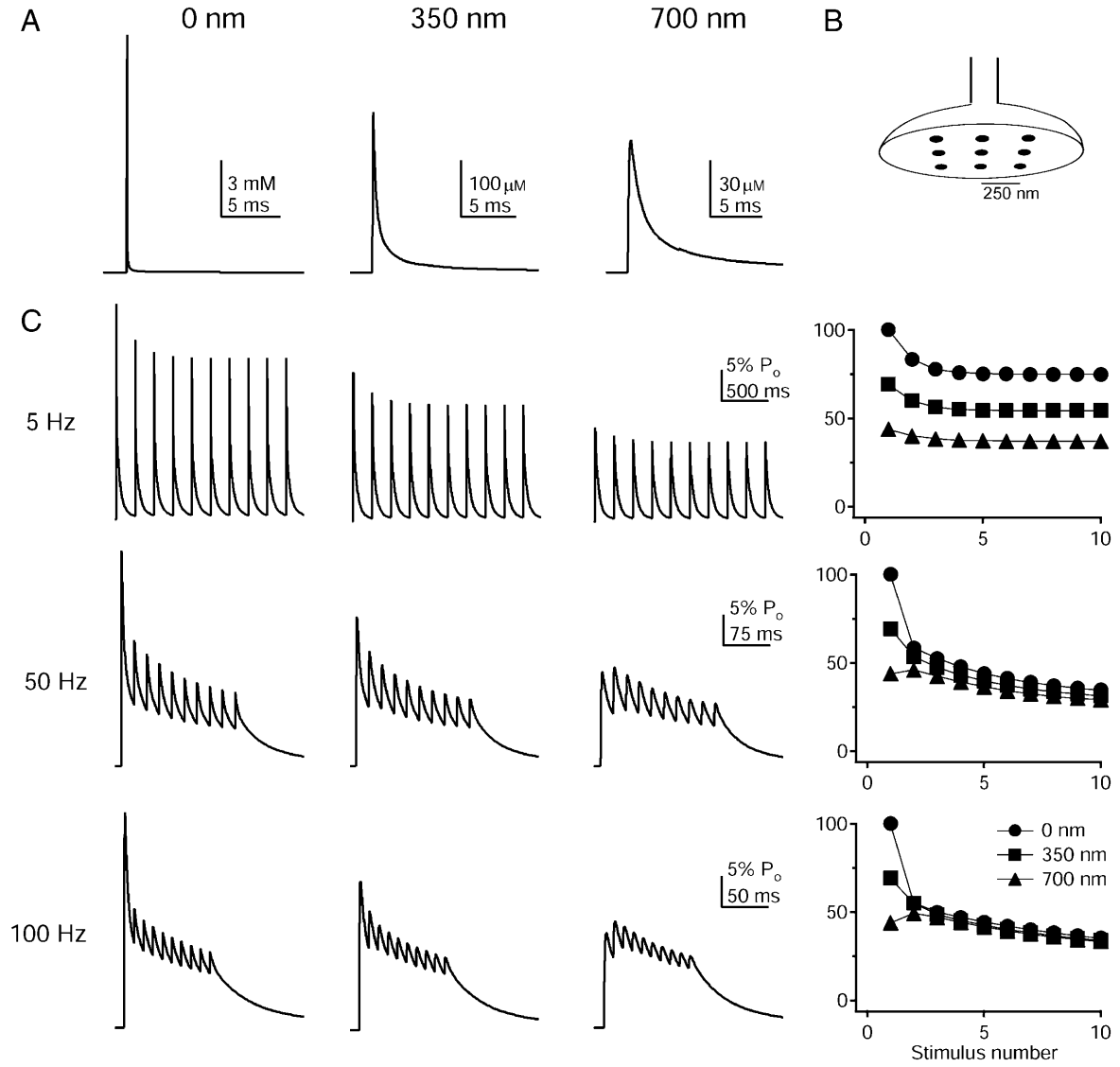

FIGURE 6 Simulations of responses of GABA$_A$ receptors to complex transients of transmitter. (*A*) Simulated concentration transients predicted by diffusion in the synaptic cleft to distances 0, 350, and 700 nm from the site of vesicle fusion. (*B*) Schematic of a multiple-site Purkinje bouton with 3 × 3 array of presynaptic densities arranged as in the simulation (postsynaptic densities not shown), with a minimum intersite distance of 250 nm. (*C*) Trains of simulated responses to the repeated application at 5, 50, or 100 Hz of the concentration profiles of GABA at 0, 350, and 700 nm (*left*). The peak responses, normalized to the first peak of the 0-nm train, plotted versus stimulus number for each frequency (*right*).

array, the maximal distance between release sites (from any corner to the diagonally opposite corner) is ~700 nm. We therefore simulated concentration transients at 0, 250, 350, 500, 550, and 700 nm from the site of release, which approximate all possible distances that transmitter can diffuse laterally from a release site to any postsynaptic site in the array (see Materials and Methods). (Note that the 14-nm cleft width is also incorporated into the simulations). For receptors 350 nm and 700 nm from a release site, the predicted concentration transients peak at 285 μM (for 350 nm) or 70 μM (for 700 nm; Fig. 6 *A*, *middle* and *right*). After ~2 ms, the concentration equilibrates across the cleft, reaching ~30 μM at all sites beneath the bouton.

Next, we used these concentration profiles to drive the kinetic model of cerebellar nuclear GABA$_A$ receptors. Fig. 6 *C* illustrates the modeled responses to 5-Hz, 50-Hz, and 100-Hz trains of simulated release, recorded 0, 350, or 700 nm away from the simulated release site, and peak currents at each distance are plotted against stimulus number. Several attributes of the simulated responses are consistent with the experimental results obtained by varying GABA concentration and stimulus frequency. First, the simulated responses are smaller at more distant sites where the peak concentration is lower. Second, the relative decrement in response amplitude during a train is greatest closest to the release site, i.e., with exposure to the highest concentrations

of transmitter. Third, the rate of decrement of peak currents increases with stimulus frequency only for receptors close to the release site, which detect the highest peak concentration of GABA. The simulations also predict that a substantial response is elicited from receptors as far as 700 nm from the release site. In IPSCs recorded in slices, the baseline-to-peak rise time is 1.35 ms (Telgkamp et al., 2004). Although the simulated current evoked 700 nm from the release site rises more slowly, peaking at 2.7 ms, it reaches 88% of its maximal value after 1.35 ms, suggesting that activation of such distant receptors may contribute to the peak of the IPSC. In fact, the relative contribution of distant receptors increases with repeated stimuli; by the 10th stimulus at 50 or 100 Hz, the peak currents of close and distant receptors are virtually indistinguishable (Fig. 6 *C*, *right*).

To describe the contribution of distant receptors more precisely, we addressed the oversimplification of Fig. 6, namely, the fact that the simulated release events occurred repeatedly from the same site on all 10 stimuli, even at 100 Hz. Such repeated release from the same site is unlikely to occur physiologically, since the vesicular release probability (P_v) per presynaptic stimulus is usually <1 at real synapses, and since the time course of replenishment is rarely briefer than the 10-ms interstimulus interval (Zucker and Regehr, 2002). We therefore simulated probabilistic release from multiple-site boutons, in which the presynaptic site(s) that release GABA can change from stimulus to stimulus, so that the concentration profile at any given postsynaptic density will vary according to which site(s) release. In our previous studies, short-term synaptic depression at the corticonuclear synapse could be well described by multiple-site boutons with a P_v of 0.1 and a bi-exponential time course of vesicle replenishment ($\tau_{refill,\ fast}$ and $\tau_{refill,\ slow}$) with time constants of 150 ms (50%) and 15 s (Telgkamp et al., 2004). These estimates of P_v and τ_{refill}, however, were derived from simulations that ignored receptor desensitization and differential activation of close and distant postsynaptic sites. Nevertheless, to test the roles of receptor desensitization and of distant receptors in generating the pattern of synaptic responses, we retained these values and simulated responses to 100-Hz, 10-pulse trains of stimuli applied to a nine-site bouton.

Because this stochastic multiple-site model allows different presynaptic sites to release on each of the 10 stimuli, successive trains of stimuli evoke different patterns of release. In addition, because of the relatively long replenishment time, presynaptic sites deplete during each train, and vesicle fusion becomes less likely with each stimulus. Thus, trains of simulated currents can depress as a result of presynaptic depletion as well as postsynaptic desensitization. Fig. 7 *A* illustrates four sample trials, indicating the site(s) that released on each stimulus as numbers representing the position of each release site in the 3×3 array of sites on the bouton. (The corresponding postsynaptic sites are numbered in Fig. 7 *B*, *stim 1*). On Trial 1, the first stimulus evoked release from presynaptic site 2, the second stimulus evoked no release, the third stimulus evoked release from site 7, and so forth. In Fig. 7 *B*, for every stimulus that evoked release on Trial 1, each of the nine postsynaptic sites is color-coded according to its distance from the site of release, such that the color indicates the peak GABA concentration reached at

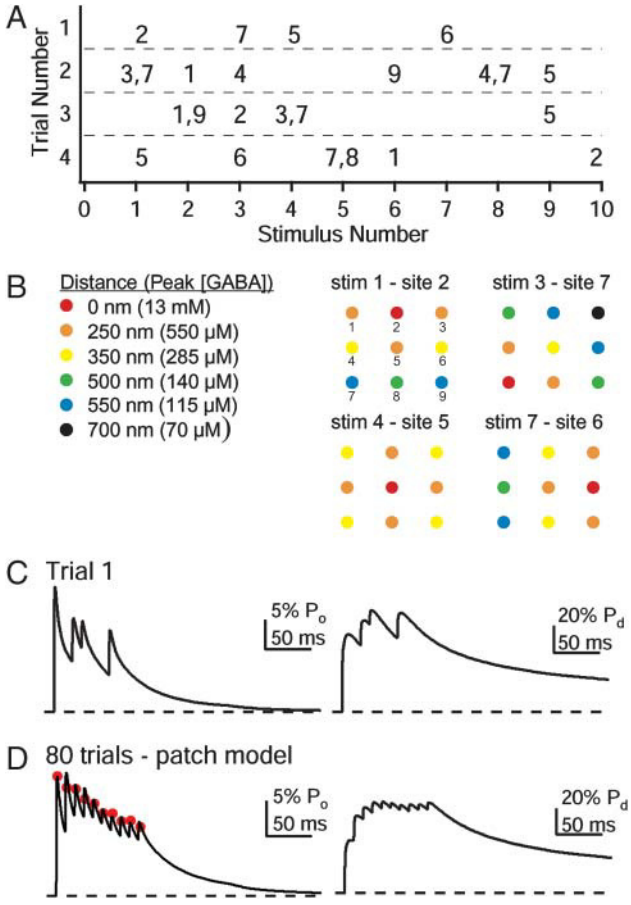

FIGURE 7 Simulations of responses to probabilistic release from multiple-site boutons. (*A*) Four example trials from a stochastic model of vesicle release during 100-Hz stimulation of the presynaptic bouton. The *x* axis is stimulus number, representing action potential invasion of a Purkinje bouton. In each row (*Trial number*), the numbers indicate which of the nine presynaptic site(s), if any, released a vesicle on each stimulus. (*B*) Schematic representation of the 3×3 array of postsynaptic sites, with numbers indicating the nine presynaptic release sites. The color of each postsynaptic site indicates its distance from the presynaptic site of vesicle fusion and therefore the peak GABA concentration reaching that location. The four arrays show the pattern of peak GABA concentrations for each release event in Trial 1 in *A*, and include cases in which GABA is released from a side (stimulus *1* and stimulus *7*), a corner (stimulus *3*), or the middle (stimulus *4*) of the array. (*C*) Simulated open probability (P_o), across all nine postsynaptic densities, resulting from the sequence of release events in Trial 1 (*left*) as well as the mean occupancy of desensitized states (P_d) across all postsynaptic sites (*right*). (*D*) Mean P_o (*left*) and mean P_d (*right*) across all postsynaptic sites averaged over 80 trials of simulated release. For comparison, the mean peaks from 100-Hz trains of IPSCs recorded in slices are superimposed on the simulated traces (*red circles*; data from Telgkamp and Raman, 2002).

each site. For each stimulus, the open probabilities (P_o) at all nine postsynaptic sites were averaged to give the mean P_o for all receptors opposite the bouton. The resulting P_o for Trial 1, along with the mean occupancy of desensitized states (P_d), is illustrated in Fig. 7 *C*. To estimate the postsynaptic responses and accumulation into desensitized states that would result from activation of several boutons, 80 trials were averaged, and the simulated postsynaptic currents are shown in Fig. 7 *D* (*left*).

The profile of depression of the mean simulated postsynaptic currents is noticeably distinct from any of the trains in Fig. 6 *C*, in which GABA was released from the same site on all 10 stimuli. Specifically, with the multiple-site model, the first few responses were of roughly the same amplitude, unlike the responses to repeated release from 0- or 350-nm away. In this regard, the responses to multiple-site release resemble the responses to repeated release from 700 nm. In the multiple-site model, however, the extent of depression late in the train was considerably greater than that predicted by trains of repeated release from 700 nm away. Although much of this depression resulted from the depletion of presynaptic sites, desensitization also contributed to decreasing the response amplitude of receptors. Plotting the summed occupancy of DA_1, DA_2f, and DA_2s illustrates that, after three stimuli, ~65% of the receptors accumulated into desensitized states, and the total occupancy of desensitized states fluctuated by only ~5% for the remainder of the train (Fig. 7 *D*, *right*).

The two main features of the multiple-site simulation—namely a slow onset of depression and a moderate extent of depression—resemble the IPSCs evoked at 100 Hz in cerebellar nuclear cells in slices (Telgkamp and Raman, 2002; Telgkamp et al., 2004). For comparison, the peak amplitudes of a train of IPSCs are superimposed on the simulated currents of Fig. 7 *D* (*red symbols*, data from Telgkamp and Raman, 2002). Despite the similarity in the peak amplitudes of the measured IPSCs and the simulated postsynaptic responses, however, the kinetics of the modeled and experimental data differ substantially. Specifically, the simulated postsynaptic currents have a slow component of decay that is not detectable in synaptically evoked IPSCs, which decay with a single-exponential time constant of ~5.5 ms at 31°C at −40 mV (Telgkamp et al., 2004; Fig. 8 *A*, *black* and *blue traces*). This discrepancy may arise, not from a failure of the kinetic model to replicate the properties of receptors in patches, but from differences between receptor properties in patches and at the synapse. As reported above, GABA-activated currents in patches (recorded at 0 mV) deactivate bi-exponentially, with a τ_{fast} of ~4 ms, quite close to the decay constant of the IPSC. This τ_{fast}, however, accounts for only ~70% of the decay; the τ_{slow} of deactivation of ~50 ms does not have an obvious correlate in synaptically evoked currents.

Although such slowing of GABA$_A$ receptor kinetics has been previously ascribed to the inclusion of extrasynaptic receptors in the patches (Banks and Pearce, 2000) or to voltage-dependent changes in gating at more depolarized potentials (Mellor and Randall, 1998), neither of these possibilities seems likely in our experiments. Across patches, kinetics were highly replicable, consistent with a single, dominant class of receptors. In cerebellar nuclear neurons, the majority of the somatic membrane (~70%) is apposed by inhibitory boutons (Chan-Palay, 1977; De Zeeuw and Berrebi, 1995; Garin and Escher, 2001), making excision of synaptic membrane highly likely. Consistent with this idea, application of 1 mM GABA to patches evoked large currents, with a mean amplitude of 667 ± 80 pA, ($N = 46$). Assuming single channel conductances of 20–30 pS and a driving force of 70 mV predicts 300–500 channels per patch, values that are hard to reconcile with an extrasynaptic origin. Regarding voltage-dependent kinetics, changing the holding potential of patches from 0 mV to −30 mV (the nominal voltage at which IPSCs were previously recorded) did not change the time courses of desensitization or deactivation after brief pulses ($N = 4$, $p > 0.25$, paired *t*-test).

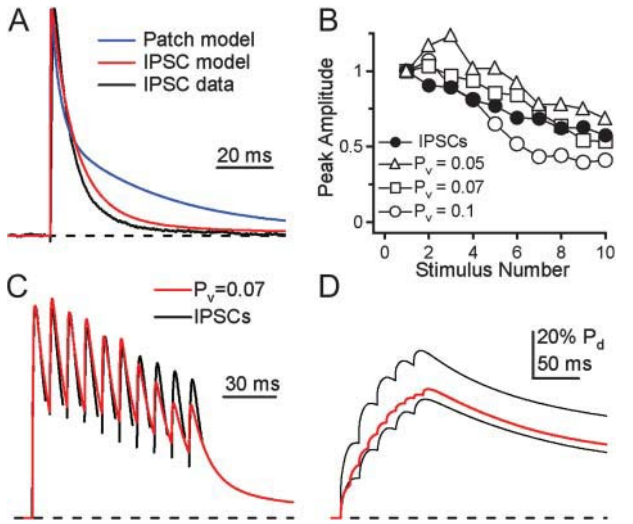

FIGURE 8 Comparison of IPSC-like model and experimentally recorded IPSCs. (*A*) Summed response of all nine postsynaptic sites to vesicle fusion in the middle of the 3 × 3 array of presynaptic sites (site 5), simulated either with the patch model (*blue*) or the IPSC-like model (*red*) of GABA$_A$ receptors. An IPSC recorded from a cerebellar nuclear neuron in a slice is plotted (*black*) for comparison (*trace* from Telgkamp et al., 2004). The peak amplitudes of all traces have been normalized. (*B*) Normalized peak responses to 100-Hz stimulation with the multiple-site model of release and the IPSC-like kinetic scheme with P_v equal to 0.05 (*open triangles*), 0.07 (*open squares*), or 0.1 (*open circles*). For comparison, the mean peak responses of IPSCs to 100-Hz stimulation are also plotted (*solid circles*; same data as in Fig. 7 *C*). (*C*) Mean of 45 trials of responses to the multiple-site model, simulated with P_v of 0.07, and the IPSC-like kinetic scheme (*red trace*). A 100-Hz train of IPSCs is superimposed for comparison (*black*; trace from Telgkamp et al., 2004). (*D*) Occupancy of desensitized states for the 45 trials of 8C (*red*). Superimposed for comparison is the P_d at a single postsynaptic site, either 0 nm (*upper black trace*) or 700 nm (*lower black trace*) from a presynaptic site releasing repeatedly at 50 Hz.

A more plausible basis for the apparent difference between patch and synaptic receptors seems to be the process of patch excision itself. Patch excision from neurons can disrupt phosphorylation, prolonging deactivation of $GABA_A$ receptors (Jones and Westbrook, 1997). A similar slowing of deactivation can be induced by pharmacological stabilization of desensitized states by neurosteroids (Zhu and Vicini, 1997). In our model, a greater stability of DA_2f is predicted to accelerate the fast phase of deactivation while increasing the percent contribution of the slow phase, because receptors that have accumulated in DA_2f are likely to reopen upon removal of GABA, before ligand unbinds (Jones and Westbrook, 1995). Evidence for a stabilization of desensitization upon patch excision from cerebellar nuclear neurons is supported by comparison of our whole-cell and patch data. Like patches, whole-cell currents desensitized bi-exponentially; however, the τ_{fast} in whole cells (5.0 $\pm$ 0.3 ms) accounted for only 40% of the decay in whole cells, versus 70% in patches. Although this increased contribution of τ_{fast} in patches may in part be explained by the faster solution exchange over patches as compared to whole cells, it may also arise from a real change in the transition rates into and/or out of desensitized states.

To test whether a destabilization of desensitization in the patch model might more closely simulate IPSCs, therefore, we increased the K_d for DA_2f 25-fold. With this single change, the simulated deactivation after a 1-ms application of 1 mM GABA became dominated by a τ_{fast} of ~6 ms (accounting for 83% of the decay), matching the decay time of the IPSC quite well (Fig. 8 *A*, *black* and *red lines*). Although we could not rule out that the stability of other states, such as DA_2s, was also modified by patch excision, no other changes were necessary to mimic the IPSC. Moreover, the destabilization of DA_2f in the IPSC-like model had minimal effects on the EC_{50} for ligand (28-μM patch versus 31-μM IPSC-like model). Likewise, the quasi-equilibrium occupancy of desensitized states at the end of 10-pulse trains of direct release decreased only slightly (86% patch versus 80% IPSC-like model), since this parameter is dominated by DA_2s. The greatest difference between the two kinetic schemes, besides the deactivation kinetics that motivated the change, was that the peak P_o evoked by any dose of ligand nearly doubled in the IPSC-like model. Thus, it seemed reasonable to use the patch data, refined by the destabilization of fast desensitization suggested by the IPSC data, as a template for a working kinetic model of synaptic receptors.

We therefore repeated the simulations of responses to the multiple-site model of release with the IPSC-like model. With P_v at 0.1 and the recovery time constants of 150 ms and 15 s, the simulated responses to 100-Hz trains depressed to a greater extent than experimentally recorded IPSCs (Fig. 8 *B*, *solid* and *open circles*). This observation suggests that either the values of P_v and recovery timecourse require adjustment, or that other factors, such as facilitation and Ca-dependent acceleration of vesicle replenishment, strongly shape the profile of depression (Wang and Kaczmarek, 1998; Dittman et al., 2000). To test whether the pattern of synaptically recorded depression could be replicated by a simple decrease in the vesicular release probability, we repeated the simulations with P_v values of 0.07 and 0.05. As with the P_v of 0.1, the overall profile of simulated currents retained the characteristic corticonuclear pattern of a slow-onset, incomplete synaptic depression. The modest decreases in P_v, however, not only reduced the absolute amplitude of the first simulated current in the train, but were also sufficient to increase the relative amplitudes of simulated currents toward the end of the train (Fig. 8 *B*, *triangles* and *squares*). In fact, the P_v of 0.07 was particularly effective at replicating the amplitudes as well as the kinetics of the experimentally recorded IPSCs (Fig. 8 *C*). Importantly, the simulated currents decayed by nearly 50% in the 10-ms interstimulus interval, much like evoked IPSCs (Telgkamp and Raman, 2002). Additionally, with the IPSC-like kinetic scheme, the onset of desensitization was slower than with the patch kinetic scheme, although it still reached a quasi-equilibrium value near 65% during the 100-Hz train (Fig. 8 *D*, *red line*). Since, in this simulation, postsynaptic sites were exposed to transmitter on approximately half of the 10 stimuli at 100 Hz, the levels of desensitization resulting from repetitive release at 50 Hz from 0 and 700 nm, simulated with the IPSC-like kinetic scheme, were superimposed (*black lines*). Comparison of these records indicates that the multiple-site model predicts ~15% less total receptor desensitization than does the model of direct, repeated release. Thus, spillover-mediated activation of $GABA_A$ receptors may allow a high-frequency activation of receptors while limiting the overall level of desensitization.

DISCUSSION

These data offer one explanation for how corticonuclear synapses maintain a robust inhibitory signal even at presynaptic firing rates at or exceeding 100 Hz (Telgkamp and Raman, 2002). The challenge at these synapses arises because high firing rates tend to increase presynaptic depletion of release-ready vesicles as well as postsynaptic desensitization of receptors, both of which are predicted to weaken inhibition. Our earlier studies suggested that the morphology of Purkinje boutons appear adapted for a local spillover-mediated transmission, which may maximize inhibitory efficacy by allowing a single release event to activate several postsynaptic densities, while preserving the availability of release-ready vesicles via a low vesicular release probability (Telgkamp et al., 2004). The present experiments provide evidence that corticonuclear synapses fulfill two other important criteria necessary for effective spillover-mediated transmission to occur. First, diffusion modeling suggests that a significant concentration of transmitter can reach neighboring postsynaptic sites. Second, the

receptor properties suggest that $GABA_A$ receptors up to 700 nm from a presynaptic active zone can bind transmitter and open, rather than desensitize, sufficiently rapidly to contribute to the peak postsynaptic current.

Spillover-mediated synaptic transmission

In general, spillover occurs as transmitter diffuses and activates receptors other than those at the postsynaptic density immediately opposite the presynaptic site of release. Although metabotropic receptors can clearly be activated in this way (Isaacson et al., 1993; Scanziani et al., 1997; Scanziani, 2000; Mitchell and Silver, 2000), whether the ionotropic receptors respond to spillover is more variable across synapses. At excitatory synapses onto hippocampal CA1 pyramidal cells, rapid uptake mechanisms and low-affinity receptors minimize spillover and its effects, indicating that most synaptic contacts are well segregated (Asztely et al., 1997; Rusakov and Kullmann, 1998; Diamond, 2001). In contrast, spillover effectively activates synaptic AMPA receptors at parallel fiber-stellate cell synapses (Carter and Regehr, 2000) and at cerebellar mossy fiber-granule cell synapses (DiGregorio et al., 2002).

At inhibitory synapses, the relation between transmitter concentration and $GABA_A$ receptor affinity often appears unsuitable for effective spillover-mediated transmission, with the exception of high-affinity, extrasynaptic $\alpha 6$ GABA receptors of cerebellar granule cells (Brickley et al., 1996; Rossi and Hamann, 1998; Hamann et al., 2002). Specifically, in many preparations, $GABA_A$ receptors are not saturated after fusion of a single vesicle (Frerking et al., 1995; Nusser et al., 1997; Galarreta and Hestrin, 1997; Perrais and Ropert, 1999; Kirischuk et al., 2002; Perrais and Ropert, 2000, but see Auger et al., 1998). Subsaturation of receptors, presumably located directly opposite release sites, makes it seem unlikely that distant receptors are activated by the even lower concentration of GABA that might reach them.

The complex ultrastructure of Purkinje terminals, which distinguishes them from many other inhibitory synapses, complicates the assessment of the occupancy of postsynaptic receptors. In this case, spillover is limited to the postsynaptic sites under a single synaptic bouton, and occupancy is likely to vary across sites. Our patch and whole-cell recordings provide an estimate of receptor sensitivity at 31–33°; the kinetic measurements permit development of a working gating scheme of the receptors; and the data on synaptic ultrastructure permits the simulation of reasonably realistic concentration transients to drive the model of receptor gating. Before using this information to compare occupancy at directly- and spillover-activated sites, however, it is worth assessing the extent to which the responses of excised patches replicate the kinetics of synaptic receptors.

Relative to other studies, $GABA_A$ receptors in cerebellar nuclear patches desensitize and deactivate quite quickly (Jones and Westbrook, 1995; Mellor et al., 2000; Kapur et al., 1999; Banks and Pearce, 2000; Hinkle and Macdonald, 2003), although similarly rapid gating has been recorded elsewhere (Galarreta and Hestrin, 1997; Zhu and Vicini, 1997; Mozrzymas et al., 2003). The gating properties in cerebellar nuclear cells are likely to result, in part, from the specific $GABA_A$ subunits expressed. The dominant subunit combination of these neurons is probably $\alpha_1\beta_2\gamma_2$L, possibly with δ-subunits (Garin et al., 2002; Gambarana et al., 1991; Laurie et al., 1992; Fritschy et al., 1994; Low et al., 2000; Boileau et al., 2003), as other subunits are either present at lower levels or absent. Interestingly, in expression systems, $\alpha_1\beta_2\gamma_2$ receptors produce currents with faster kinetics than other combinations of subunits (Verdoorn, 1994; Gingrich et al., 1995; Lavoie et al., 1997; McClellan and Twyman, 1999). In addition, the kinetics that we measured may have been accelerated by the fact that recordings were made $\sim$10° above room temperature.

Despite the relatively rapid gating, however, deactivation of $GABA_A$ receptors in cerebellar nuclear patches was measurably slower than the decay of experimentally recorded IPSCs. Although slow gating in hippocampal pyramidal patches results from sampling extrasynaptic receptors (Banks and Pearce, 2000), this source of error appears unlikely in our preparation. As mentioned, the high density of Purkinje boutons apposed to cerebellar nuclear somata (Chan-Palay, 1977), as well as the high density of receptors per patch, makes it highly probable that excised patches are dominated by synaptic membrane. Moreover, at corticonuclear synapses, all $GABA_A$ receptors opposite any bouton, whether or not they correspond to anatomically distinguishable postsynaptic densities, must be included as synaptic receptors. In other words, only receptors that are not apposed by the bouton, but are located on the other side of the transporter-expressing astrocytic processes, qualify as extrasynaptic receptors. Additionally, contrary to the prediction from a high density of extrasynaptic receptors with unusual properties, blockade of GABA transporters in slices failed to change kinetics of IPSCs (Telgkamp et al., 2004).

Pursuing the hypothesis that the patches indeed contained synaptic receptors, therefore, an alternative explanation for the slow deactivation kinetics is that patch-excision modified receptor kinetics. In the worst-case scenario, the properties of patch receptors might bear no systematic relation to those at intact synapses. Comparisons of patch data to whole-cell responses to exogenous or synaptically released GABA, however, suggested that the stability of the doubly-liganded, fast desensitized state (DA_2f) was simply increased by patch excision. Although we cannot verify that all other transitions remained constant, our experiments gave no evidence that they changed. Interestingly, in several channel types, including $GABA_A$ receptors, NMDA receptors, Na channels,

and K channels, gating kinetics change in patches in a manner consistent with stabilization of desensitized/inactivated states (Rosenmund and Westbrook, 1993; Jones and Westbrook, 1997; Shcherbatko et al., 1999; Chen et al., 2000). Importantly, in our model, a simple destabilization of DA_2f changed patchlike responses into IPSC-like responses.

Saturation, activation, and desensitization of $GABA_A$ receptors at corticonuclear synapses

Therefore, by measuring the occupancy of the unbound, singly-liganded, and doubly-liganded states in the IPSC-like model, we can estimate receptor occupancy, as well as entry into desensitized states. Directly opposite the release site, only 1.5% of receptors are unliganded (*C*) at the time of the peak current, and 5% are in the singly-bound (*CA*) state, consistent with near-saturation of receptors. In contrast, 700 nm from the release site, only approximately half of the receptors are doubly liganded at the peak of the current, with 41% of the receptors in C, and 16% in CA_1. Thus, although many postsynaptic sites opposite a bouton may bind ligand, the receptor occupancy is likely to vary across sites.

Specifically, in the model, the high receptor occupancy directly opposite the release site elicits a large current (peak $P_o \sim 74\%$), but receptors then desensitize, reducing the number of receptors available at that site to respond to successive stimuli. At spillover-activated sites, subsaturation of receptors evokes a smaller current (peak $P_o \sim 31\%$ for a 700-nm distance). A smaller fraction of the receptors at that site will accumulate into desensitized states, however, producing a lower P_d after a single stimulus. Because each postsynaptic site has only an 11% chance of a direct hit every time a release occurs from a nine-site bouton, sites are more commonly activated indirectly than directly, leading to moderate occupancy, moderate open probabilities, as well as moderate desensitization. Thus, despite the fast desensitization that often accompanies rapid gating, the subsaturating concentrations of GABA resulting from spillover delay the onset of postsynaptic depression, permitting a subset of receptors to remain responsive even at high rates of presynaptic signaling.

These factors are relevant in light of the high-frequency activity typical of corticonuclear transmission. Action potentials propagate along Purkinje axons at rates as high as 250 spikes/s (Khaliq and Raman, 2005). Purkinje synaptic terminals can be effective at translating these impulses into chemical signals only if vesicle depletion can be limited, and cerebellar nuclear neurons can detect the GABA only if their receptors remain responsive to high rates of inhibitory input. Our data suggest that corticonuclear synapses may fulfill these requirements via a low vesicular release probability from multiple-site boutons coupled with postsynaptic receptors that appear adapted for detection of spillover of GABA.

We are grateful to Dr. Petra Telgkamp for recording the IPSCs reproduced in Fig. 8, and to Zayd Khaliq, Tina Grieco, and Teresa Aman for helpful discussions.

Supported by National Institutes of Health No. NS39395 and the Searle Scholars Program (to I.M.R.).

REFERENCES

Afshari, F. S., K. Ptak, Z. M. Khaliq, T. M. Grieco, N. T. Slater, D. R. McCrimmon, and I. M. Raman. 2004. Resurgent Na currents in four classes of neurons of the cerebellum. *J. Neurophysiol.* 92:2831–2843.

Asztely, F., G. Erdemli, and D. M. Kullmann. 1997. Extrasynaptic glutamate spillover in the hippocampus: dependence on temperature and the role of active glutamate uptake. *Neuron.* 18:281–293.

Auger, C., S. Kondo, and A. Marty. 1998. Multivesicular release at single functional synaptic sites in cerebellar stellate and basket cells. *J. Neurosci.* 18:4532–4547.

Banks, M. I., and R. A. Pearce. 2000. Kinetic differences between synaptic and extrasynaptic $GABA_A$ receptors in CA1 pyramidal cells. *J. Neurosci.* 20:937–948.

Boileau, A. J., T. Li, C. Benkwitz, C. Czajkowski, and R. A. Pearce. 2003. Effects of γ_{2S} subunit incorporation on $GABA_A$ receptor macroscopic kinetics. *Neuropharmacology.* 44:1003–1012.

Brickley, S. G., S. G. Cull-Candy, and M. Farrant. 1996. Development of a tonic form of synaptic inhibition in rat cerebellar granule cells resulting from persistent activation of $GABA_A$ receptors. *J. Physiol.* 15:753–759.

Bruns, D., D. Riedel, J. Klingauf, and R. Jahn. 2000. Quantal release of serotonin. *Neuron.* 28:205–220.

Carter, A. G., and W. G. Regehr. 2000. Prolonged synaptic currents and glutamate spillover at the parallel fiber to stellate cell synapse. *J. Neurosci.* 20:4423–4434.

Chan-Palay, V. 1977. Cerebellar Dentate Nucleus. Organization, Cytology, and Transmitters. Springer-Verlag, Berlin, Germany.

Chen, J., V. Avdonin, M. A. Ciorba, S. H. Heinemann, and T. Hoshi. 2000. Acceleration of P/C-type inactivation in voltage-gated K^+ channels by methionine oxidation. *Biophys. J.* 78:174–187.

Clements, J. D., R. A. Lester, G. Tong, C. E. Jahr, and G. L. Westbrook. 1992. The time course of glutamate in the synaptic cleft. *Science.* 258:1498–1501.

Colquhoun, D., P. Jonas, and B. Sakmann. 1992. Action of brief pulses of glutamate on AMPA/kainate receptors in patches from different neurones of rat hippocampal slices. *J. Physiol.* 458:261–287.

De Zeeuw, C. I., and A. S. Berrebi. 1995. Postsynaptic targets of Purkinje cell terminals in the cerebellar and vestibular nuclei of the rat. *Eur. J. Neurosci.* 7:2322–2333.

Diamond, J. S., and C. E. Jahr. 1995. Asynchronous release of synaptic vesicles determines the time course of the AMPA receptor-mediated EPSC. *Neuron.* 15:1097–1107.

Diamond, J. S. 2001. Neuronal glutamate transporters limit activation of NMDA receptors by neurotransmitter spillover on CA_1 pyramidal cells. *J. Neurosci.* 21:8328–8338.

DiGregorio, D. A., Z. Nusser, and R. A. Silver. 2002. Spillover of glutamate onto synaptic AMPA receptors enhances fast transmission at a cerebellar synapse. *Neuron.* 35:521–533.

Dittman, J. S., A. C. Kreitzer, and W. G. Regehr. 2000. Interplay between facilitation, depression, and residual calcium at three presynaptic terminals. *J. Neurosci.* 20:1374–1385.

Frerking, M., S. Borges, and M. Wilson. 1995. Variation in GABA mini amplitude is the consequence of variation in transmitter concentration. *Neuron.* 15:885–895.

Fritschy, J. M., J. Paysan, A. Enna, and H. Mohler. 1994. Switch in the expression of rat $GABA_A$-receptor subtypes during postnatal development: an immunohistochemical study. *J. Neurosci.* 14:5302–5324.

Galarreta, M., and S. Hestrin. 1997. Properties of $GABA_A$ receptors underlying inhibitory synaptic currents in neocortical pyramidal neurons. *J. Neurosci.* 17:7220–7227.

Gambarana, C., C. E. Beattie, Z. R. Rodriguez, and R. E. Siegel. 1991. Region-specific expression of messenger RNAs encoding $GABA_A$ receptor subunits in the developing rat brain. *Neuroscience.* 45:423–432.

Garin, N., and G. Escher. 2001. The development of inhibitory synaptic specializations in the mouse deep cerebellar nuclei. *Neuroscience.* 105: 431–441.

Garin, N., J. P. Hornung, and G. Escher. 2002. Distribution of postsynaptic $GABA_A$ receptor aggregates in the deep cerebellar nuclei of normal and mutant mice. *J. Comp. Neurol.* 447:210–217.

Gingrich, K. J., W. A. Roberts, and R. S. Kass. 1995. Dependence of the $GABA_A$ receptor gating kinetics on the α-subunit isoform: implications for structure-function relations and synaptic transmission. *J. Physiol.* 489:529–543.

Hamann, M., D. J. Rossi, and D. Attwell. 2002. Tonic and spillover inhibition of granule cells control information flow through cerebellar cortex. *Neuron.* 33:625–633.

Hestrin, S. 1992. Activation and desensitization of glutamate-activated channels mediating fast excitatory synaptic currents in the visual cortex. *Neuron.* 5:991–999.

Hinkle, D. J., and R. L. Macdonald. 2003. β-subunit phosphorylation selectively increases fast desensitization and prolongs deactivation of $\alpha1\beta1\gamma2$L and $\alpha1\beta3\gamma2$L $GABA_A$ receptor currents. *J. Neurosci.* 17: 11698–11710.

Hines, M. L., and N. T. Carnevale. 1997. The NEURON simulation environment. *Neural Comput.* 9:1179–1209.

Isaacson, J. S., J. M. Solis, and R. A. Nicoll. 1993. Local and diffuse synaptic actions of GABA in the hippocampus. *Neuron.* 10:165–175.

Jones, M. V., and G. L. Westbrook. 1995. Desensitized states prolong $GABA_A$ channel responses to brief agonist pulses. *Neuron.* 15:181–191.

Jones, M. V., and G. L. Westbrook. 1997. Shaping of IPSCs by endogenous calcineurin activity. *J. Neurosci.* 17:7626–7633.

Kapur, J., K. F. Haas, and R. L. Macdonald. 1999. Physiological properties of $GABA_A$ receptors from acutely dissociated rat dentate granule cells. *J. Neurophysiol.* 81:2464–2471.

Khaliq, Z. M., and I. M. Raman. 2005. Axonal propagation of simple and complex spikes in cerebellar Purkinje neurons. *J. Neurosci.* 25:454–463.

Kirischuk, S., J. D. Clements, and R. Grantyn. 2002. Presynaptic and postsynaptic mechanisms underlie paired pulse depression at single GABAergic boutons in rat collicular cultures. *J. Physiol.* 543:99–116.

Laurie, D. J., P. H. Seeburg, and W. Wisden. 1992. The distribution of 13 $GABA_A$ receptor subunit mRNAs in the rat brain. II. Olfactory bulb and cerebellum. *J. Neurosci.* 12:1063–1076.

Lavoie, A. M., J. J. Tingey, N. L. Harrison, D. B. Pritchett, and R. E. Twyman. 1997. Activation and deactivation rates of recombinant $GABA_A$ receptor channels are dependent on α-subunit isoform. *Biophys. J.* 73:2518–2526.

Low, K., F. Crestani, R. Keist, D. Benke, I. Brunig, J. A. Benson, J. M. Fritschy, T. Rulicke, H. Bluethmann, H. Mohler, and U. Rudolph. 2000. Molecular and neuronal substrate for the selective attenuation of anxiety. *Science.* 290:131–134.

Mellor, J. R., and A. D. Randall. 1998. Voltage-dependent deactivation and desensitization of GABA responses in cultured murine cerebellar granule cells. *J. Physiol.* 506:377–390.

McClellan, A. M., and R. E. Twyman. 1999. Receptor system response kinetics reveal functional subtypes of native murine and recombinant human $GABA_A$ receptors. *J. Physiol.* 515:711–727.

Mellor, J. R., and A. D. Randall. 2001. Synaptically released neurotransmitter fails to desensitize postsynaptic $GABA_A$ receptors in cerebellar cultures. *J. Neurophysiol.* 85:1847–1857.

Mellor, J. R., W. Wisden, and A. D. Randall. 2000. Somato-synaptic variation of $GABA_A$ receptors in cultured murine cerebellar granule cells: investigation of the role of the $\alpha6$ subunit. *Neuropharmacology.* 39:1495–1513.

Mitchell, S. J., and R. A. Silver. 2000. GABA spillover from single inhibitory axons suppresses low-frequency excitatory transmission at the cerebellar glomerulus. *J. Neurosci.* 20:8651–8658.

Mozrzymas, J. W., A. Barberis, K. Mercik, and E. D. Zarnowska. 2003. 2003. Binding sites, singly bound states, and conformation coupling shape GABA-evoked currents. *J. Neurophysiol.* 89:871–883.

Nielsen, T. A., D. A. DiGregorio, and R. A. Silver. 2004. Modulation of glutamate mobility reveals the mechanism underlying slow-rising AMPAR EPSCs and the diffusion coefficient in the synaptic cleft. *Neuron.* 42:757–771.

Nusser, Z., S. Cull-Candy, and M. Farrant. 1997. Differences in synaptic $GABA_A$ receptor number underlie variation in GABA mini amplitude. *Neuron.* 19:697–709.

Otis, T., S. Zhang, and L. O. Trussell. 1996. Direct measurement of AMPA receptor desensitization induced by glutamatergic synaptic transmission. *J. Neurosci.* 16:7496–7504.

Overstreet, L. V., M. V. Jones, and G. L. Westbrook. 2000. Slow desensitization regulates the availability of synaptic $GABA_A$ receptors. *J. Neurosci.* 20:7914–7921.

Perrais, D., and N. Ropert. 1999. Effect of Zolpidem on miniature IPSCs and occupancy of postsynaptic $GABA_A$ receptors in central synapses. *J. Neurosci.* 19:578–588.

Perrais, D., and N. Ropert. 2000. Altering the concentration of GABA in the synaptic cleft potentiates miniature IPSCs in rat occipital cortex. *Eur. J. Neurosci.* 12:400–404.

Raman, I. M., A. E. Gustafson, and D. Padgett. 2000. Ionic currents and spontaneous firing in neurons isolated from the cerebellar nuclei. *J. Neurosci.* 20:9004–9016.

Raman, I. M., and L. O. Trussell. 1995. The mechanism of α-amino-3-hydroxy-5-methyl-4-isoxazolepropionate receptor desensitization after removal of glutamate. *Biophys. J.* 68:137–146.

Ribak, C. E., W. M. Tong, and N. C. Brecha. 1996. Astrocytic processes compensate for the apparent lack of GABA transporters in the axon terminals of cerebellar Purkinje cells. *Anat. Embryol. (Berl.).* 194:379–390.

Rosenmund, C., and G. L. Westbrook. 1993. Calcium-induced actin depolymerization reduces NMDA channel activity. *Neuron.* 10:805–814.

Rossi, D. J., and M. Hamann. 1998. Spillover-mediated transmission at inhibitory synapses promoted by high affinity $\alpha6$-subunit $GABA_A$ receptors and glomerular geometry. *Neuron.* 20:783–795.

Rusakov, D. A., and D. M. Kullmann. 1998. Extrasynaptic glutamate diffusion in the hippocampus: ultrastructural constraints, uptake, and receptor activation. *J. Neurosci.* 18:3158–3170.

Scanziani, M., P. A. Salin, K. E. Vogt, R. C. Malenka, and R. A. Nicoll. 1997. Use-dependent increases in glutamate concentration activate presynaptic metabotropic glutamate receptors. *Nature.* 385:630–634.

Scanziani, M. 2000. GABA spillover activates postsynaptic $GABA_B$ receptors to control rhythmic hippocampal activity. *Neuron.* 25:673–681.

Shcherbatko, A., F. Ono, G. Mandel, and P. Brehm. 1999. Voltage-dependent sodium channel function is regulated through membrane mechanics. *Biophys. J.* 77:1945–1959.

Sodickson, D. L., and B. P. Bean. 1996. $GABA_B$ receptor-activated inwardly rectifying potassium current in dissociated hippocampal CA3 neurons. *J. Neurosci.* 16:6374–6385.

Telgkamp, P., D. E. Padgett, V. A. Ledoux, C. S. Woolley, and I. M. Raman. 2004. Maintenance of high-frequency transmission at Purkinje to cerebellar nuclear synapses by spillover from boutons with multiple release sites. *Neuron.* 41:113–126.

Telgkamp, P., and I. M. Raman. 2002. Depression of inhibitory synaptic transmission between Purkinje cells and neurons of the cerebellar nuclei. *J. Neurosci.* 22:8447–8457.

Thach, W. T. 1968. Discharge of cerebellar neurons during rapidly alternating arm movements in the monkey. *J. Neurophysiol.* 31:785–797.

Trussell, L. O., and G. D. Fischbach. 1989. Glutamate receptor desensitization and its role in synaptic transmission. *Neuron.* 3:209–218.

Verdoorn, T. A. 1994. Formation of heteromeric γ-aminobutyric acid type A receptors containing two different α-subunits. *Mol. Pharmacol.* 45:475–480.

Wagner, D. A., and M. V. Jones. 2004. A potent uncompetitive antagonist of the $GABA_A$ receptor is released by Tygon micro-bore tubing. Program No. 844.17. Abstract Viewer/Itinerary Planner. Society for Neuroscience, Washington, DC, E-pub.

Wang, L.-Y., and L. Kaczmarek. 1998. High-frequency firing helps replenish the readily releasable pool of synaptic vesicles. *Nature.* 394:384–388.

Zhu, W. J., and S. Vicini. 1997. Neurosteroid prolongs $GABA_A$ channel deactivation by altering kinetics of desensitized states. *J. Neurosci.* 17:4022–4031.

Zucker, R. S., and W. G. Regehr. 2002. Short-term synaptic plasticity. *Annu. Rev. Physiol.* 64:355–405.